Phytoplankton blooms and fish recruitment rate: Effects of spatial distribution

V. N. Biktashev [a,b,*] J. Brindley [a]

[a] *Department of Applied Mathematics, University of Leeds, Leeds LS2 9JT, UK*

[b] *Department of Mathematical Sciences, M&O Building, Peach street, University of Liverpool, Liverpool L69 7ZL, UK*

Abstract

We consider the spatio-temporal dynamics of a spatially-structured generalisation of the phytoplankton-zooplankton-fish larvae model system proposed earlier (Biktashev, Brindley & Horwoord 2003, James, Pitchford & Brindley 2003). In contrast to Pitchford and Brindley (2001), who were concerned with small scale patchiness (i.e. 1–10 m), on which the (stochastic) raptorial behaviour of individual larvae is important, we address here the much larger scale "patchy" problems (i.e. 10–100 km), on which both larvae and plankton may be regarded as passive tracers of the fluid motion, dispersed and mixed by the turbulent diffusion processes. In particular, we study the dependence of the fish recruitment on carrying capacities of the plankton subsystem and on spatiotemporal evolution of that subsystem with respect to the larvae hatching site(s). It is shown that the main features found both in the non-structured and age-structured spatially uniform models are observed in the spatially structured case, but that spatial effects can significantly modify the overall quantitative outcome.

Spatial patterns in the metamorphosed fish distribution are a consequence of quasi-local interaction of larvae with plankton, in which the dispersion of larvae by large scale turbulent eddies plays little part due to the relatively short time scale of the larvae development. As a result, in a strong phyto/zooplankton subsystem, with fast reproduction rate and large carrying capacity of phytoplankton and high conversion ratio of zooplankton, recruitment success depends only on the localisation and timing of the hatching with respect to the plankton patches. In a weak phyto/zooplankton system, with slow reproduction rate and small carrying capacity of phytoplankton and low conversion ratio of zooplankton, the larvae may significantly influence the evolution of the plankton patches, which may lead to non-trivial cooperative effects between different patches of larvae. However, in this case, recruitment is very low.

* Corresponding author. Address: Department of Mathematical Sciences, M&O Building, Peach street, University of Liverpool, Liverpool L69 7ZL, UK

Running head: Phytoplankton and fish recruitment

Send proofs to: V.B. Biktashev, Applied Mathematics, M&O Building, Peach street, University of Liverpool, Liverpool L69 7ZL, UK

E-mail: vnb@liv.ac.uk

Contact telephone: (0151) 794 4004

Contact address: as above

Fax: (0151) 794 4061

1 Introduction

Zooplankton, broadly defined for our purpose as grazers of phytoplankton, comprise a vital link between primary phytoplankton production and fish populations. Most fish at larvae stage, and many in their adult form, feed on the zooplankton grazers, typical examples being the North Sea cod and haddock, whose larvae include the *Calanus* species as a staple part of their diet (Cushing and Horwood, 1994; Heath and Gallego, 1998), and, at the other extreme, the baleen whales of the Southern Ocean, whose main diet is krill (Miller and Hampton, 1989). Zooplankton populations are also vital to the "biological pump", carrying carbon to the deep ocean through skeletal sinking.

A striking feature of oceanic plankton distributions is their spatial variation in population density (Bainbridge, 1957; Steele, 1978; Venrick, 1990). This patchiness is evident on all scales, sometimes related in an obvious way to physical features of the fluid motion such as eddies or fronts (Abraham, 1998; Flierl and Davis, 1993; Martin and Richards, 2001; McGillicuddy Jr and Robinson, 1997; Oschlies and Garçon, 1998; Strass, 1992), in other cases bearing no such clear forcing mechanism. In these latter cases it is often presumed that biological processes inherent to the population dynamics are important in producing the patchy distributions (de Roos et al., 1998; Gurney and Veitch, 2000; Folt and Burns, 1999). Observational evidence for the patchiness of phytoplankton is abundant and relatively easy to obtain, e.g. by satellite imaging (Siegel et al., 1999). Data on zooplankton distributions, vital for evaluating theoretical modeling of the dynamics, are much scarcer and more elusive, depending on direct measurement obtained from research cruise programmes (The PRIME Community, 2001; Oschlies et al., 2000).

Growth of the zooplankton population is dependent on availability of phytoplankton to graze, and a number of simplified mathematical models of their interrelated population dynamics have been proposed, e.g. (Steele and Henderson, 1981, 1992a,b; Truscott and Brindley, 1994). Most have taken the form of ODEs, representing only time evolution, but several have attempted to model also the spatial variation of population, e.g. (Steele, 1978; Pitchford and Brindley, 2001; Matthews and Brindley, 1997). Success has been limited, and crucial tests for most of these models have yet to be defined and evaluated against observation.

In this paper our concern is with the effects of spatio-temporal inhomogeneity in larval food supply on the recruitment to adult states of fish larvae, and in particular we wish to evaluate strategies for larvae distribution in space or time which might optimize that recruitment. In contrast to Pitchford and Brindley (2001), who were concerned with the effect of patchiness on such small scales that the individual (stochastic) swimming of larvae was important, we focus here on much larger space scales, on which turbulent "eddy velocities", represented in an eddy diffusion coefficient, are much larger than any larval swimming velocities (Okubo, 1980). Thus we assume that phytoplankton, zooplankton and larvae are all carried passively by the large scale

fluid velocity field. We consider a very simple plankton population model (Truscott and Brindley, 1994), coupled to a larvae evolution model (Cushing and Horwood, 1994) and examine the extent to which various egg laying strategies might exploit this system. To this end, we consider two sets of initial and boundary conditions on the plankton distributions, each leading to a travelling wavelike bloom, and carry out numerical experiments for various timings and magnitudes of larvae hatching.

The results exhibit a strong dependence on the peak hatching rate, related to the initial stock of larvae, the timing of hatching relative to the timing of any plankton bloom, and, particularly, on the phytoplankton "carrying capacity", related of course to nutrient supply and strength of irradiation. Recruitment shows a dramatic fall-off when this carrying capacity falls below some "critical" value, whatever the size of the initial stock or the timing. Dependence on the other parameters of the earlier plankton (Truscott and Brindley) and recruitment (Cushing and Horwood) models is much milder; the vital feature, perhaps unsurprisingly, is that a plankton bloom is triggered.

2 The model

2.1 Dynamic variables

Dynamic variables of the model are P, phytoplankton biomass concentration, Z, zooplankton biomass concentration, N and B, larvae number and biomass concentrations respectively, and F, the biomass concentration of the metamorphosed fish. All dynamic variables depend on time t and on one (x) or two (x, y) spatial dimensions. The spatial domain was an interval $x \in [0, x_{\max}]$ with $x_{\max} = 100\,\mathrm{km}$ in the 1D case, and a rectangle $(x, y) \in [0, x_{\max}] \times [0, y_{\max}]$ with $x_{\max} = 100\,\mathrm{km}$, $y_{\max} = 30\,\mathrm{km}$ in the 2D case. The larvae biomass was chosen as a dynamic variable instead of the larvae average weight, to allow a simplified description of the larvae diffusion. All the species, except the metamorphosed fish, were assumed to be diffusing in space. The main transport process was assumed to be passive (turbulent) diffusion, which is therefore taken equal for all three species. This assumption is appropriate for spatial scales of $\sim 10\,\mathrm{km}$ or larger; for scales of, say, $\sim 10\,\mathrm{m}$ the swimming and raptorial behaviour of individual larvae become important (Pitchford and Brindley, 2001) and the assumption of equal passive diffusion is inappropriate. Since the average weight is an intensive characteristic it cannot be described by a diffusion equation, so we used larvae biomass, which is an extensive characteristic, and expressed the dynamic equations accordingly. Otherwise, the model is identical to that used in Biktashev et al. (2003) and James et al. (2003), up to a few insignificant computational details.

As is well known (Okubo, 1980), the effective diffusion coefficient in the sea, due to the nature of turbulent diffusion, depends on the scale of phenomenon considered. However, the model used in this study can be easily rescaled to

an arbitrary diffusion coefficient, D, by a corresponding change of the spatial scales ($l \propto D^{1/2}$), which means that the absolute value of the diffusion coefficient does not have any major significance for the character of the results. We used $D = 0.864\,\mathrm{km}^2/\mathrm{d} = 10^5\,\mathrm{cm}^2/\mathrm{s}$, which according to Okubo (1980), corresponds to the scale of 10 km, i.e. consistent with the size of model area, and agreeing with Talbot's (Talbot, 1976) value for diffusivity in tidal areas.

2.2 Evolution equations

Phytoplankton dynamics are assumed to be logistic, with predation by the zooplankton:

$$\partial P/\partial t = r_P P(1 - P/P_{\max}) - G(P)Z + D\nabla^2 P, \tag{1}$$

where the grazing intensity $G(P)$ is Holling type 3:

$$G(P) = r_Z P^2/(P_*^2 + P^2). \tag{2}$$

Zooplankton dynamics express the grazing of phytoplankton, and loss to non-specific mortality and to the predation by the larvae:

$$\partial Z/\partial t = Z(\gamma G(P) - \mu_Z) - R(W, Z)N + D\nabla^2 Z, \tag{3}$$

where $R(W, Z)$ is the daily ration of an average larva. This ration cannot exceed the amount of zooplankton a larva can catch in one day. This amount can be estimated by the volume that can be searched by a larva of weight W, which is empirically approximated as kW^ν, times the density of the zooplankton Z. On the other hand, the daily ration cannot exceed the larva's metabolic demand, calculated as a ratio of its energy needs, empirically $Wr_L + \sigma W^n$, of which Wr_L represent maximal possible weight gain in a day and σW^n energy losses, over the efficiency of the food conversion, empirically $(\beta_{\max} - (\beta_{\max} - \beta_{\min})\exp(-jW))$. The actual ration is taken to be the lesser of the two,

$$R(W, Z) = \min\left(kW^\nu Z, \frac{Wr_L + \sigma W^n}{(\beta_{\max} - (\beta_{\max} - \beta_{\min})\exp(-jW))}\right), \tag{4}$$

and the current average larva weight is calculated as

$$W = B/N, \tag{5}$$

where B and N are biomass and number concentration of larvae per unit volume.

The local dynamics of the average larva weight is given by the balance between the benefit from its ration and the metabolic loss, thus its rate of change, W',

is given by

$$W' = R(W, Z)(\beta_{\max} - (\beta_{\max} - \beta_{\min}) \exp(-jW)) - \sigma W^n. \tag{6}$$

The local dynamics of the larvae number concentration, apart from the hatching, which is assumed instant and simulated as initial conditions, always leads to a loss, N', where

$$\begin{aligned} N' = -N \Bigg[& \frac{\mu_L}{1 + bA} + C_S \exp\left(-\frac{\nu_S W'}{\sigma W^n}\right) \\ & + C_A \, \theta\left(\frac{A - A_T}{\Delta_A}\right) + C_W \, \theta\left(\frac{W - W_T}{\Delta_W}\right) \Bigg], \end{aligned} \tag{7}$$

due to predation (the first term), starvation (the second term) and metamorphosis stipulated by the weight and age of the larvae (the third and the fourth terms respectively). In (7), A is the age of the larvae, i.e. the time after the hatching moment,

$$A = t - t_h, \tag{8}$$

θ is the threshold function, defined as

$$\theta(x) = \frac{1}{2}(1 + \tanh x),$$

metamorphosis age and weight are $A_T \pm \Delta_A$ and $W_T \pm \Delta_W$ respectively, and C_A and C_W determine corresponding maximum metamorphosis rates.

The local dynamics of larvae weight and number concentration are then incorporated into the spatiotemporal dynamics of the larvae concentration and biomass concentration, to give

$$\partial N/\partial t = N' + D\nabla^2 N, \tag{9}$$

$$\partial B/\partial t = NW' + WN' + D\nabla^2 B, \tag{10}$$

which differs from the original (Cushing and Horwood, 1994) model by the diffusion terms. These "reaction-diffusion" equations are written in this form because the larval biomass is an extensive property, as opposed to the average individual larva weight, which is intensive, and so its "diffusion" would not make any sense.

The final dynamic variable, the biomass F, of the metamorphosed fish, was calculated as a result of the process of metamorphosis, without any assumptions about its further dynamics and diffusion:

$$\partial F/\partial t = N \left[C_A \theta\left(\frac{A - A_T}{\Delta_A}\right) + C_W \theta\left(\frac{W - W_T}{\Delta_W}\right) \right]. \tag{11}$$

The initial and boundary conditions for this system of equations are explained further where the results of the numerical experiments are presented. In terms of final conditions, we are interested both in spatial distribution of the metamorphosed fish, i.e. $F(t_{\max}, x)$, and in total success of fish recruitment, defined in terms of the total biomass of metamorphosed fish,

$$\Sigma_F = \frac{1}{x_{\max}} \int_0^{x_{\max}} F(t_{\max}, x)\, \mathrm{d}x \tag{12}$$

and similarly for two spatial dimensions. We divide the integral here by the domain size $x_{\max}$ to get a quantity of the same dimensionality as in Cushing and Horwood (1994), i.e. the biomass concentration.

Here we have taken no account of advection by larger scale oceanic processes, but note that recent results (Neufeld et al., 2002) have indicated its potential for enhancement and spread of initially localised blooms by oceanic stirring processes.

2.3 Selected parameter sets

The default values of parameters, as well as standard initial values of the dynamic variables, are specified in the tables in the Appendix. Of all the parameters, in different experiments we varied three key parameters of the phyto-zooplankton subsystem: r_P, phytoplankton maximal growth rate; $P_{\max}$, phytoplankton carrying capacity; and γ, zooplankton grazing efficiency. These parameters differed significantly between Cushing and Horwood (1994) who considered a relatively "strong" phyto-zooplankton system, and Truscott and Brindley (1994), who considered a relatively "weak" phyto-zooplankton system. We considered these two as extreme cases, and also two intermediate cases, which we called "fair" and "modest":

	r_P	$P_{\max}$	γ
Strong	1.0	$3 \cdot 10^6$	0.15
Fair	0.7	$1 \cdot 10^6$	0.12
Modest	0.5	$5 \cdot 10^5$	0.10
Weak	0.3	$1.08 \cdot 10^5$	0.05

2.4 Local behaviour

The analysis of the local (spatially uniform) behaviour of this model is contained in our previous paper (Biktashev et al., 2003). The main findings can

be briefly summarised as follows. As well as in the model without plankton dynamics (Cushing and Horwood, 1994), recruitment tends to be a domed-shaped function of initial fish egg production (stock), where the decrease of recruitment at higher values of stock is due to depletion of the zooplankton population by larvae at an early stage. The recruitment at optimal stock strongly depends on plankton conditions, and requires "phytoplankton bloom"; outside the bloom conditions, the recruitments decreases exponentially. The timing and duration of fish egg production is important in determining recruitment through their impact on the phytoplankton bloom. Roughly, optimal timing is when the end of larval stage is close to the end of the phytoplankton bloom, if the duration of larval feeding is less than the duration of the phytoplankton bloom. A nontrivial phenomenon was initiation of the bloom by hatching larvae, via a temporal decrease of the zooplankton, triggering the prey-escape mechanism. For more details, see (Biktashev et al., 2003).

3 Results

3.1 Two types of plankton waves, and organisation of the numerical experiments

We have studied dependence of the success of fish recruitment on various features of the spatio-temporal variability of the plankton community they feed on. A simple example of this spatio-temporal variability was assumed to take the form of a propagating "wave" of high zooplankton population following the spring bloom of phytoplankton, and was considered to be supported by two alternative mechanisms, the first of which we call an invasion wave, and the second an excitation wave. These two waves are illustrated on Figure 1.

3.1.1 Invasion wave

See Figure 1(a). The initial condition takes phytoplankton at its maximum, and no zooplankton or larvae:

$$\begin{aligned} P(x,0) &= P_{\max}, \\ Z(x,0) &= 0, \\ N(x,0) &= 0, \\ B(x,0) &= 0. \end{aligned} \tag{13}$$

Zooplankton invade this initial state, modelled by imposing a constant concentration of zooplankton at one of the boundaries:

$$Z(0,t) = Z_b, \tag{14}$$

with non-flux boundary conditions in all other cases. There is some evidence that such an invasion of the northern North Sea by copepod of the species *Calanus finmarchicus* takes place when they emerge from a period of winter diapause in the deep waters of the Celtic Channel. The value of Z_b was typically chosen as $2 \cdot 10^4$; but its variation over a wide range did not lead to any noticeable differences in the behaviour. The only important requirement for this type of wave to occur was the complete absence of zooplankton in the system at $t = 0$.

Behind the invasion wave, the local dynamics brings the system to the coexistence equilibrium between phyto and zooplankton. This wave is similar to the classic KPP-Fisher (Kolmogoroff et al., 1937; Fisher, 1937) in that it is a trigger wave from an unstable equilibrium to a stable equilibrium; however it is more complicated as it involves two species, both of which diffuse.

3.1.2 Excitation wave

See Figure 1(b). Here, before the arrival of the wave, the system was in the stable coexistence equilibrium between the phyto and zooplankton:

$$\begin{aligned} P(x,0) &= P_0 > 0, \\ Z(x,0) &= Z_0 > 0, \\ N(x,0) &= 0, \\ B(x,0) &= 0, \end{aligned} \tag{15}$$

where (P_0, Z_0) are a solution of the system

$$\begin{aligned} 0 &= r_P P(1 - P/P_{\max}) - G(P)Z, \\ 0 &= Z(\gamma G(P) - \mu_Z). \end{aligned} \tag{16}$$

The wave was initiated by imposing an influx of phytoplankton at one of the boundaries, through the boundary condition

$$P(0,t) = P_b. \tag{17}$$

with non-flux boundary conditions in all other cases. This may occur when a local influx of nutrient by upwelling, or when a local increase in radiation intensity, drives a local rapid increase in phytoplankton in the region $x < 0$. The value of P_b was typically chosen to be $1.5 \cdot 10^5$, but its variation in a wide range did not lead to any noticeable differences in the behaviour. In practice, again, the exact initial and boundary conditions were not essential, as long as both phyto and zooplankton species were present initially and had small values, so that the phytoplankton bloom did not occur spontaneously, and the boundary value of P_b was large enough to initiate such a bloom. In the wave, the phytoplankton bloom happens through the prey escape mechanism, discussed in detail in Truscott and Brindley (1994).

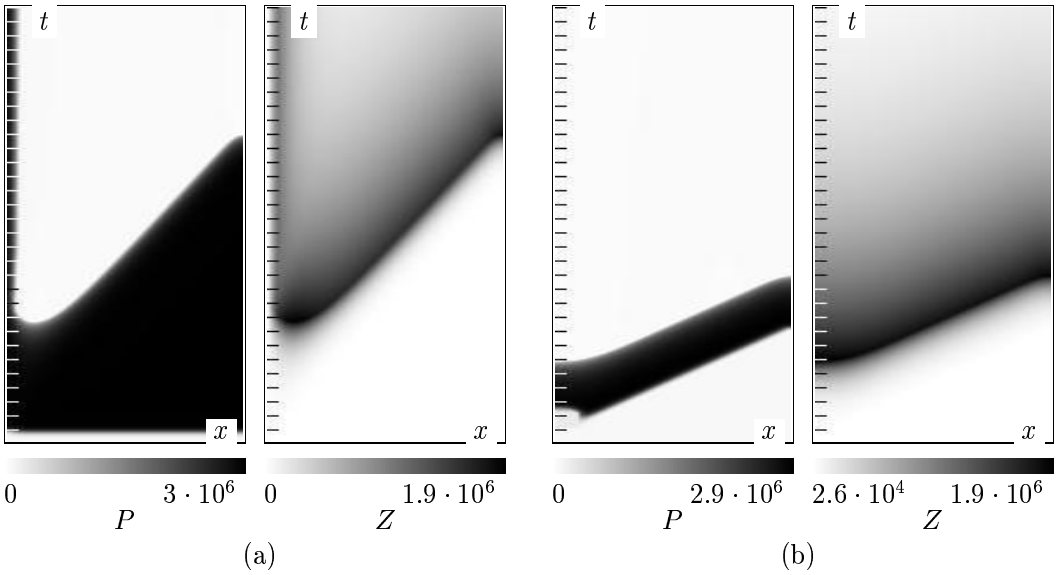

Fig. 1. The two types of plankton waves. Shown are the time-space density plots of (left panels) phytoplankton and (right panels) zooplankton. Space is horizontal, total width 100 km. Time is vertical (bottom to top), ticks in every 10 days. White is zero, black is maximum concentration. (a) Invasion wave. (b) Excitation wave.

These two types of wave are of course different idealisations of a complicated natural phenomenon. We have considered both of them to check how robust are the results.

Hatching of the larvae was simulated by imposing initial conditions for the larvae variables at $t = t_h$:

$$\begin{aligned} N(t_h, x) &= H(x), \\ B(t_h, x) &= W_0 N(t_h, x), \\ H(x) &= A_h \exp\left(-\left(\frac{x - x_h}{w_h}\right)^2\right), \end{aligned} \tag{18}$$

where x_h was typically in the middle of the computation interval, $x_h = 0.5\, x_{\max}$, and the time t_h and amplitude A_h of hatching, and the width w_h of the hatching site were varied.

3.2 Dependence of recruitment on stock and time of hatching

The dependence of recruitment on stock, measured by the maximal hatching concentration A_h and hatching time t_h, yields results for the "strong" plankton parameters as presented in Figure 2. The recruitment success is relatively insensitive to the hatching time, as long as hatching happens no sooner than the zooplankton wave arrives at the hatching site. On the other hand, the recruitment grows monotonically with increase in spawning stock, which corresponds to the abundance of the zooplankton behind the zooplankton invasion front. Only very late hatching (in the wake of the zooplankton wave) can make large spawning stock counterproductive. This corresponds to the slight downturn

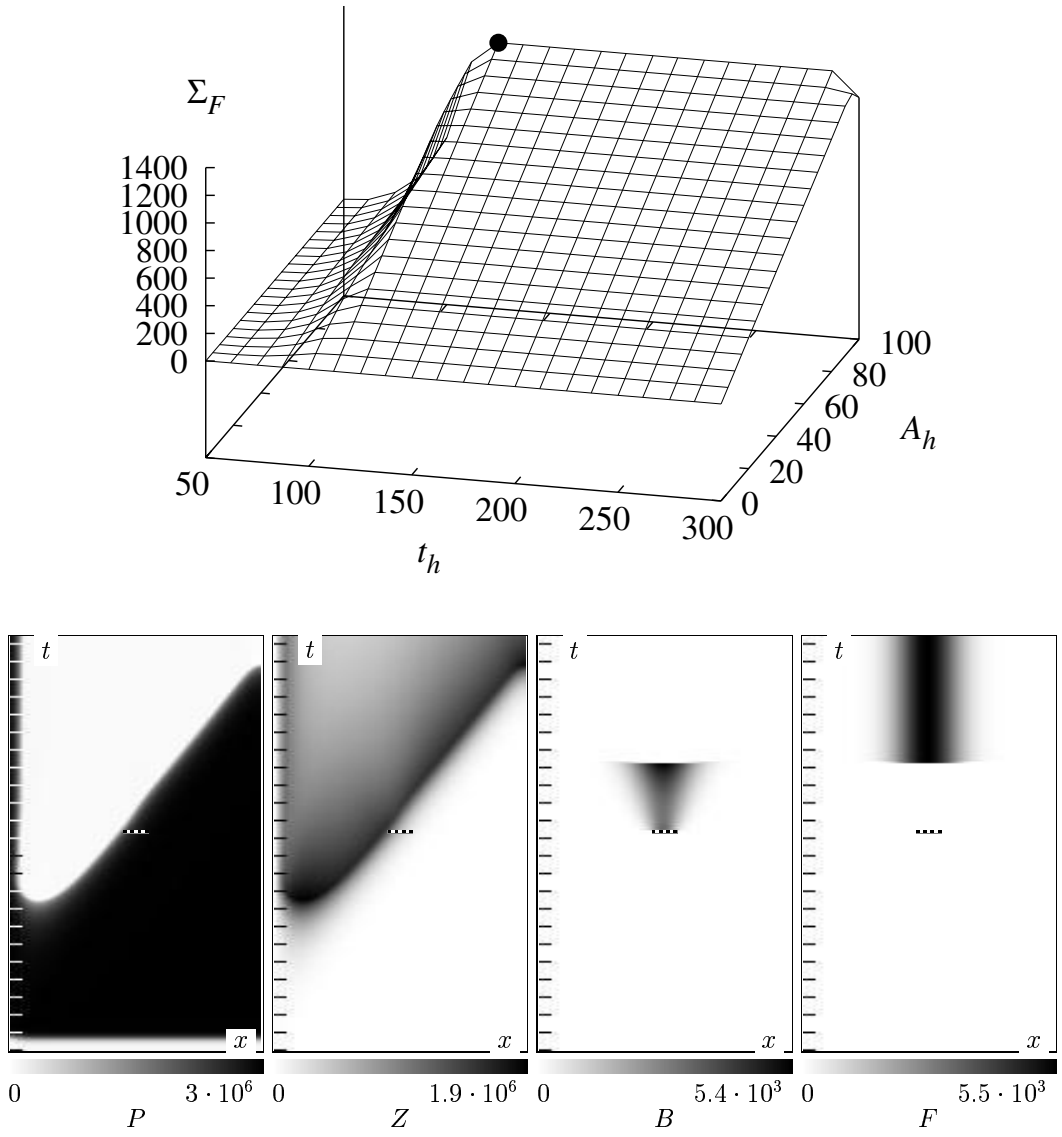

Fig. 2. Larvae development in an invasion wave in strong plankton. Upper panel: the stock-timing recruitment relationship: recruitment, i.e. the final overall metamorphosed fish biomass Σ_F as function of hatching time t_h and stock, i.e. peak hatching intensity A_h. The bullet point shows the maximum of recruitment. Lower panels: the time-space density plots of (left to right): phytoplankton, zooplankton, larvae biomass and metamorphosed fish biomass: evolution of the system corresponding to the parameter choice designated by the bullet point on the above graph. Time and space scales are as in Figure 1. The horizontal black and white stripes on the lower panels on this and subsequent figures indicate time and place of the larvae hatching; the spatial spread is defined as the interval $(x_h - w_h, x_h + w_h)$.

of the recruitment at the point $t_h = 300$, $A_h = 100$ in Figure 2; this effect is more pronounced in weaker plankton systems, discussed later. Note that larvae hatching has no effect on the evolution of the phyto-zooplankton subsystem: the zooplankton wave propagates as if without the larvae.

3.3 Dependence on the strength of the plankton

We have performed a similar series of numerical experiments for the three other sets of plankton parameters, "fair", "modest" and "weak".

In the "fair" plankton system, Figure 3, there is a definite advantage in spawning near the beginning of the zooplankton wave. The recruitment still generally grows with the stock, but, for delayed hatching times, it is far from direct proportionality, and is not even strictly monotonic. This means certain hardship for the growing larvae, i.e. their growth is limited by the success of their grazing rather than their natural growing capacity. The non-monotonicity of the stock-recruitment curves at $t_h = \text{const}$ corresponds to the Cushing-Horwood effect, whereby larvae hatched at concentration above a certain critical value eat up almost all food when young and leave too little for themselves later. Another new feature here is a significant effect of the larvae on the zooplankton wave. For the situation shown on the figure, i.e. spawning near the beginning of the zooplankton wave, the effect is seen as a temporary stop of the zooplankton wave. The maximal recruitment success in this "fair" plankton substrate is appoximately the same as in the strong plankton, but is achieved in a narrower region of parameter values.

The back influence of larvae on the plankton is even more pronounced in the "modest" plankton system, Figure 4. Here the larvae not only suspend propagation of the zooplankton wave, but almost completely destroy that wave for all the larvae development period. After larvae metamorphose, a new wave of zooplankton emerges, propagating in two directions: the backward wave is an excitation rather than invasion wave. Another new feature here is the bimodal spatial distribution of the metamorphosed fish. This is due to the same Cushing-Horwood effect: the concentration of hatched larvae near the peak of initial distribution is above the critical concentration, and so the stock-recruitment dependence there is negative. In total, this severe intraspecific competition noticeably decreases the success of fish recruitment, and makes dependence on the parameters even sharper. The bimodal shape of the 'crest' of Σ_F along A_h axis is due to the sharpness of the maximum of $\Sigma_F(t_h)$ dependence and discrete sampling on the t_h axis.

Further decrease of the phyto-zooplankton vitality almost completely precludes any fish development, Figure 5. Here the larvae demand from the very beginning exceeds the supply of the zooplankton, which leads to an almost complete extinction of both the zooplankton and larvae at the hatching site. The overall fish recruitment success in this case is microscopic, compared to the previous cases.

3.4 Dependence on the type of plankton wave

To test the sensitivity of the effects to the exact mechanisms causing the spatiotemporal variability of the zooplankton, we have repeated all the same

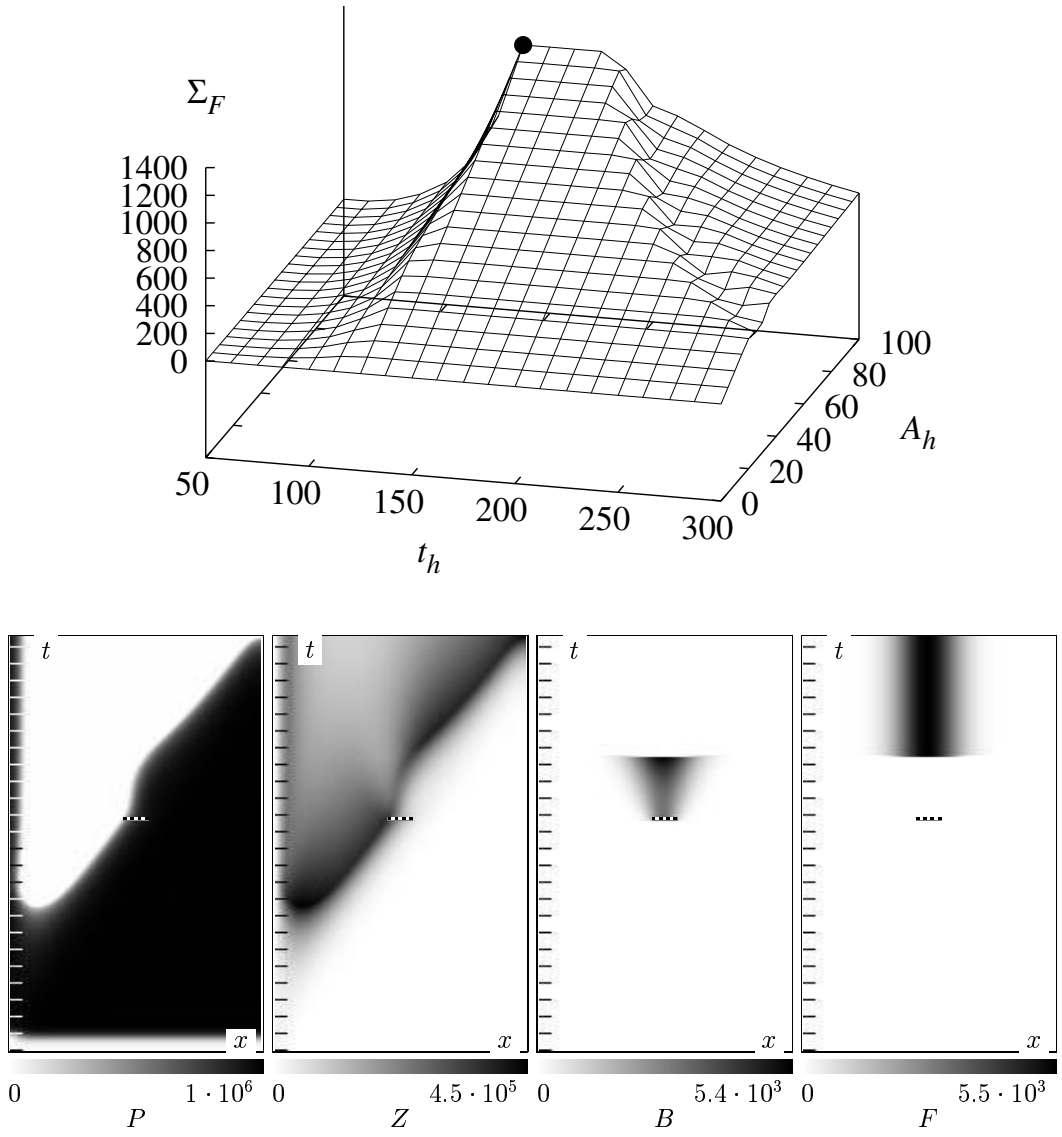

Fig. 3. Same as Figure 2, for fair plankton

numerical experiments for the excitation, rather than invasion, waves. The difference is that, in the excitation waves, the phytoplankton wave precedes the zooplankton wave, whereas in the invasion waves the phytoplankton is abundant everywhere ahead of the zooplankton wave. A quantitative difference is that an excitation wave propagates faster that an invasion wave in the same system. These differences have proved to have little effect on the larvae development, and the results of the numerics were quite similar to those in invasion waves. We present only one illustration, for the "fair" plankton parameters, Figure 6. Apart from the profile and speed of the plankton wave, the only noticeable difference is a later onset of favourable conditions for the larvae, corresponding to a later arrival of the zooplankton wave, as it starts only some time after the phytoplankton wave. Thus the difference is entirely due to the artificial procedure of imposing the spatiotemporal variability.

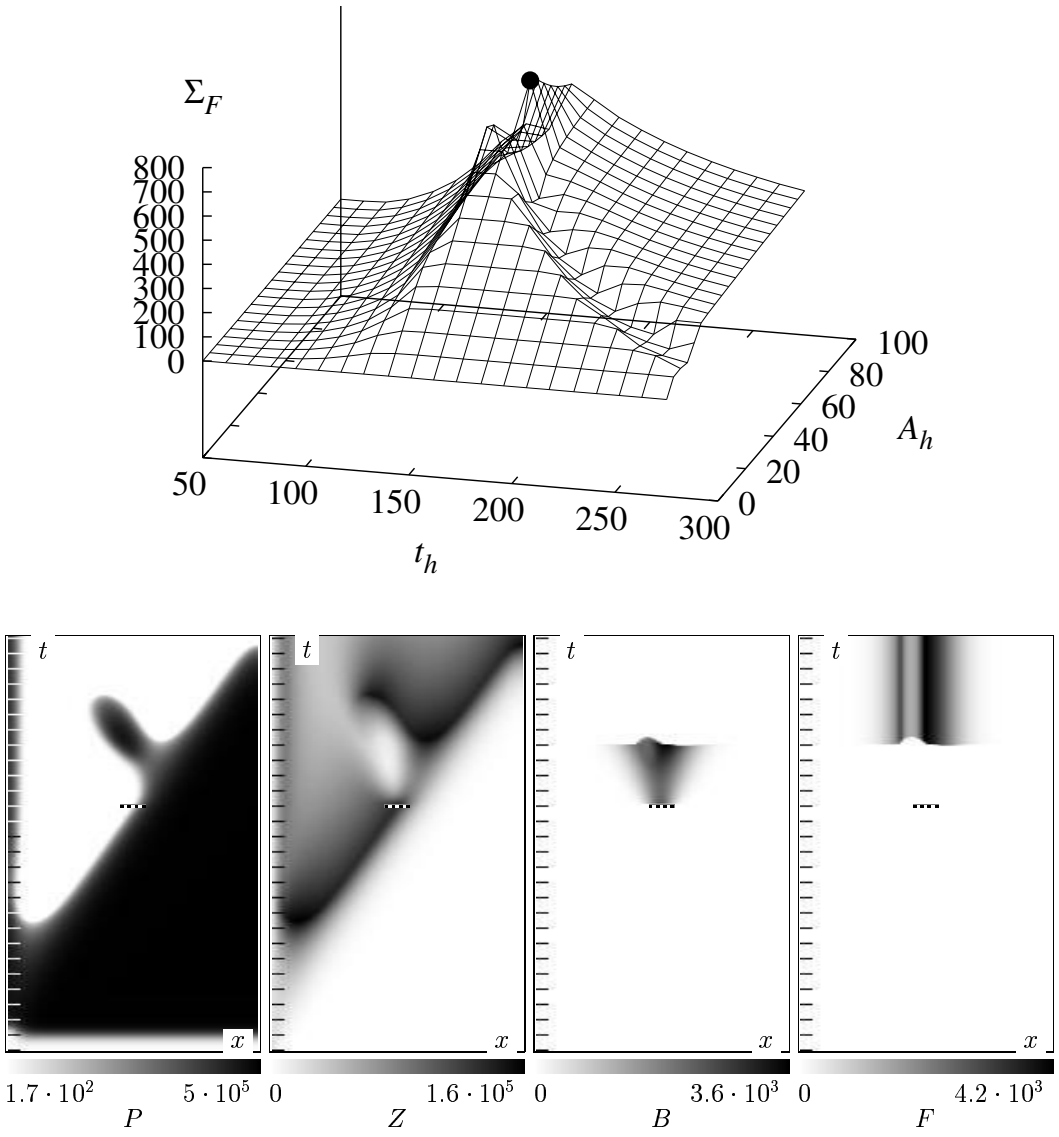

Fig. 4. Same as Figure 2, for modest plankton

3.5 Dependence on the size of the hatching site

Another set of numerical experiments was for a wider spatial distribution of hatching, with $w_h = 20\,\text{km}$, as opposed to $w_h = 5\,\text{km}$ as in the previous numerics. As one would expect, the major difference in all cases was a wider range of favourable hatching times, with approximately the same maximal recruitment values. An example is shown on Figure 7, for "modest" plankton parameters. One can see that the main characteristic features remain similar to Figure 4: the sharp maximum of recruitment dependence on hatching time (although it now comes later, especially at smaller hatching amplitudes, and is less sharp), the tendency to bimodal distribution of the metamorphosed fish (although the distribution itself is wider), and the decremental backward wave of plankton from the hatching site (although now it is much slower).

The comparison of recruitment success with different geometries of the hatch-

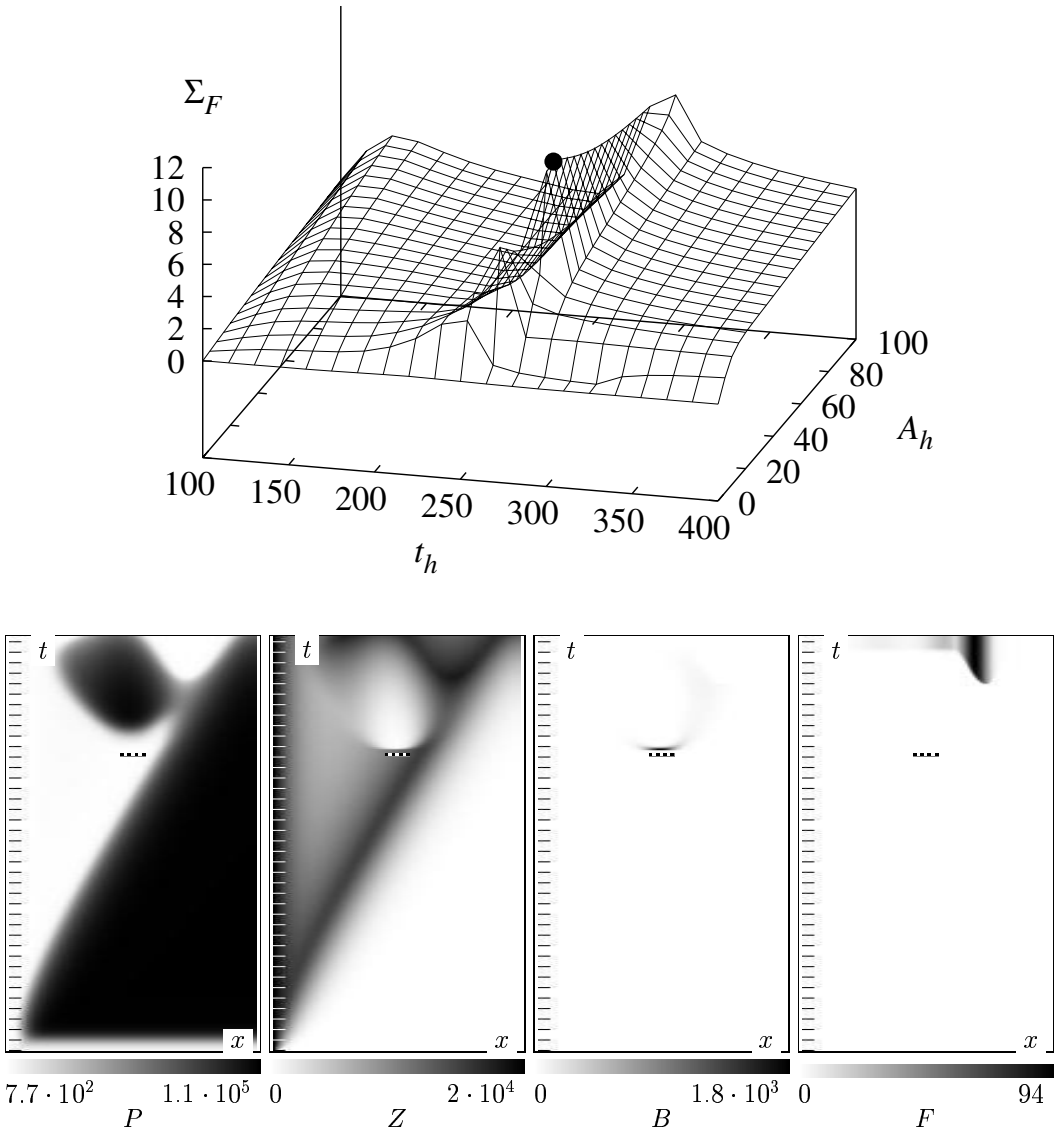

Fig. 5. Same as Figure 2, for weak plankton

ing distribution is more meaningful if we take a total hatching number,

$$\Sigma_N = \int_0^{x_{\max}} N(t_h, x)\,\mathrm{d}x, \tag{19}$$

as a measure of the spawning stock, instead of the maximal hatching intensity A_h. Using (18), this gives

$$\Sigma_N = \sqrt{\pi} A_h w_h \operatorname{erf}\left(\frac{x_{\max}}{2w_h}\right). \tag{20}$$

We present two examples of the dependences on the hatching width for controlled hatching number: Figure 8, for $\Sigma_F(\Sigma_N, w_h)$, at a fixed t_h and "modest" plankton parameters), and Figure 9, for $\Sigma_F(t_h, w_h)$, at a fixed Σ_N and "fair" plankton parameters. One can see on both graphs that dependence on the width is mainly monotonically growing, and only slightly decreasing at small

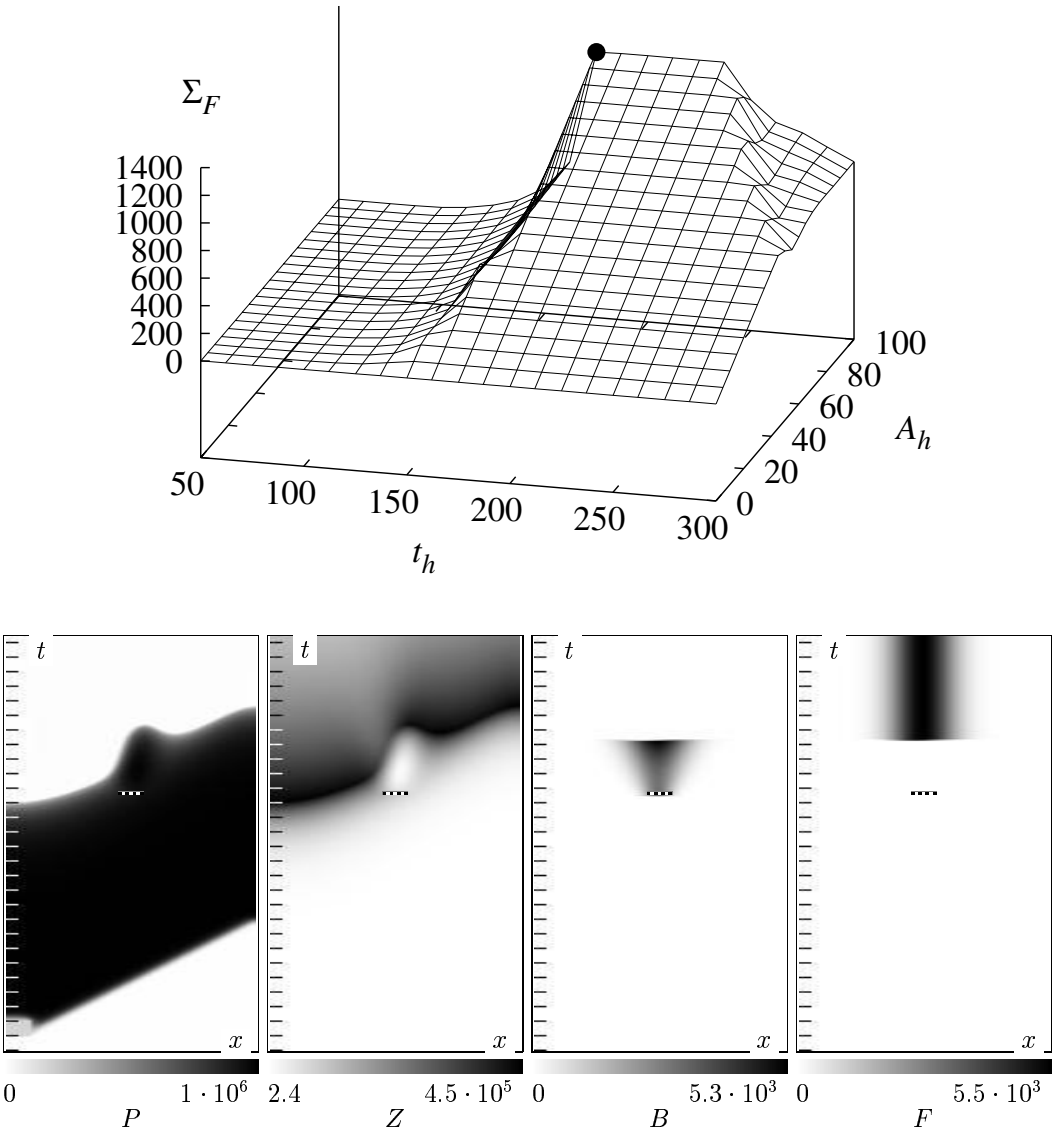

Fig. 6. Same as Figure 3 (fair plankton), for an excitation rather than invasion wave.

hatching width, nearly optimal time and stronger plankton. This shows that, generally, the dependence of larvae growth on the environment is so sharp that the chance that some larvae would hatch somewhere in favourable conditions is far more important than the number of larvae experiencing those conditions; all the more so since high concentration of larvae may be counterproductive if it exceeds the Cushing-Horwood critical value. This can be seen on the sample evolution plots on both Figures 8 and 9. In each case the parameters were chosen to be slightly suboptimal and hatching was after the advent of the zooplankton wave. In both cases the limiting factor for the larvae growth was not only limited abundance of the zooplankton, but also an excessive intial concentration of larvae in certain places, leading to their starvation later in their development, and retarded metamorphosis with lower biomass.

An extensive search through the parameter space for all four plankton parameter sets and a 3-parameter grid of values of w_h, t_h and Σ_N, not presented here to save space, has indicated that this behaviour is quite typical, and, at a given total hatching number, the homogeneous distribution of hatching

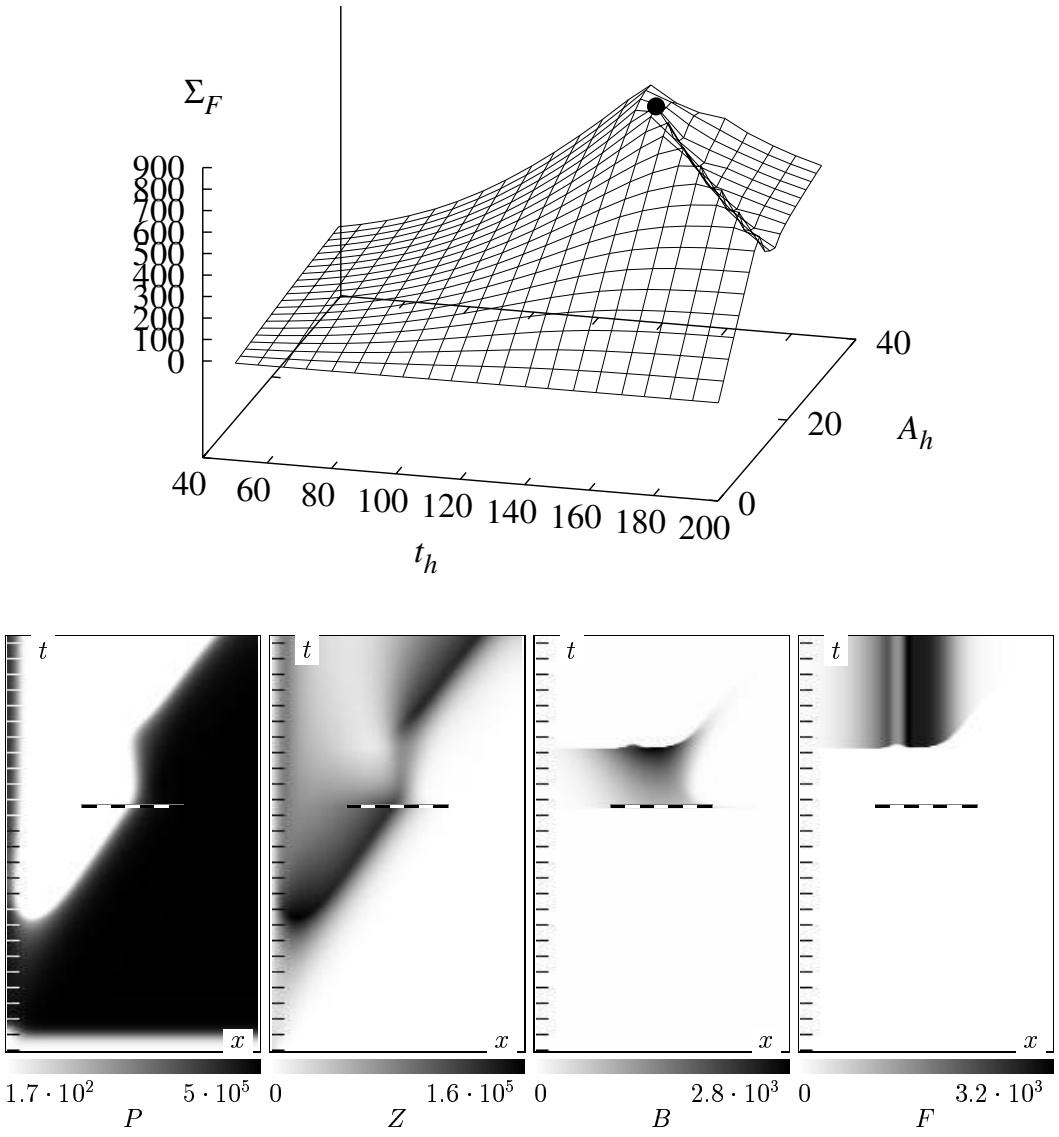

Fig. 7. Similar to Figure 4, but for a wider hatching area ($w_h = 20$km).

intensity is either optimal or, at worst, slightly suboptimal.

3.6 Interaction of hatching cohorts via the plankton waves

In our model, hatching of larvae can trigger a wave of phytoplankton bloom via a temporary reduction of the zooplankton. This can only happen in a relatively weak phyto/zooplankton subsystem. Moreover, the increase in zooplankton following the bloom is delayed in time and/or displaced with respect to the hatching event that triggered it, and therefore is unlikely to be beneficial for this particular batch of larvae. It can, however, be utilised by another batch of larvae later in time and in another place, where and when the zooplankton component of the wave initiated by the first batch arrives. To explore this possibility, we have modified the larvae initial conditions (18) to the following:

$$N(t_{hj} + 0, x) = N(t_{hj} - 0, x) + H_j(x),$$

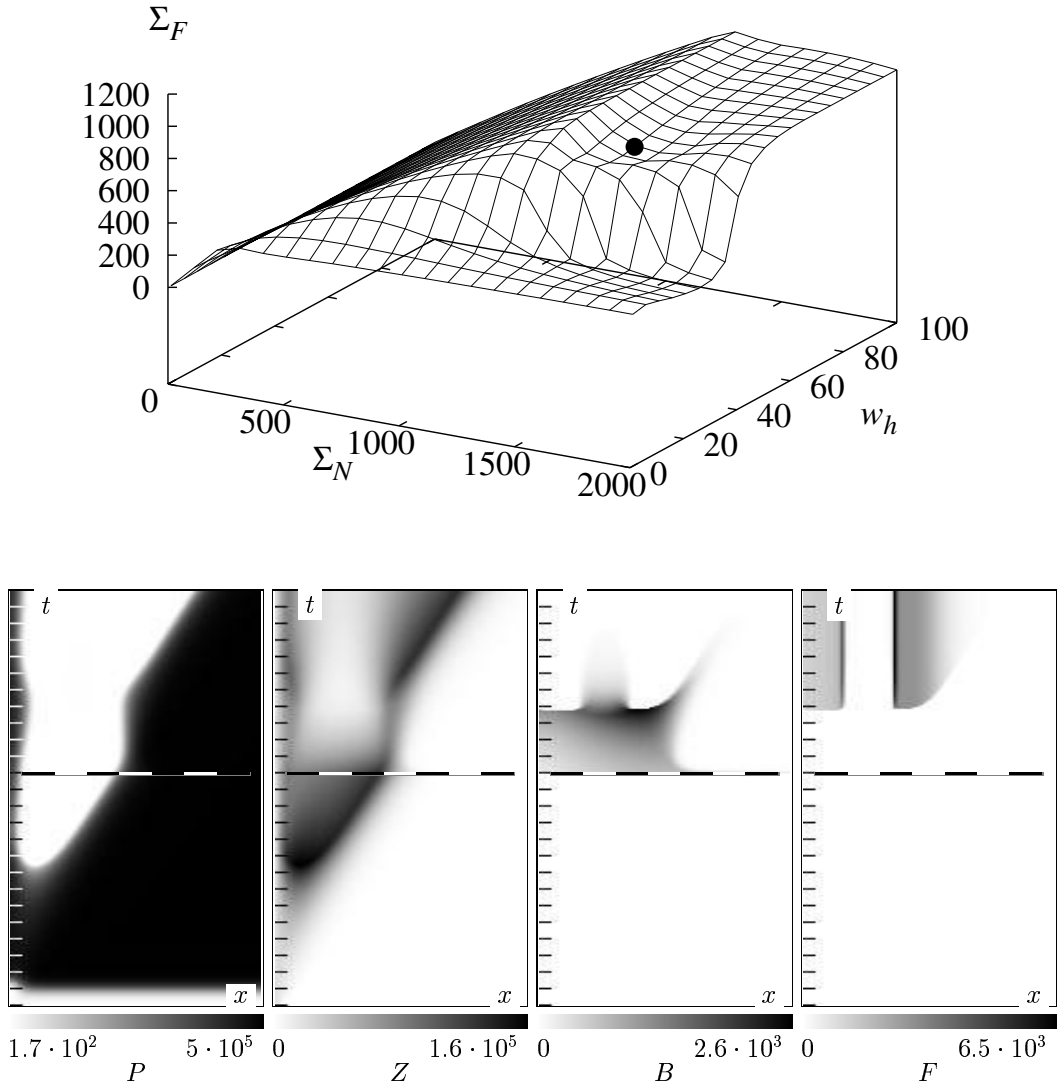

Fig. 8. Recruitment biomass, as function of total hatching numbers ("stock") Σ_N and width w_h, for a selected hatching time, $t_h = 140$. "Modest" plankton parameters. Lower panels: evolution of the system corresponding to the parameter choice designated by the filled circle on the above graph.

$$B(t_{hj}+0,x) = B(t_{hj}-0,x) + W_0 H_j(x),$$
$$H_j(x) = A_{hj} \exp\left(-\left(\frac{x-x_{hj}}{w_{hj}}\right)^2\right),$$
$$(j=1,2), \tag{21}$$

i.e. as two similar events with different parameters, occurring at different times $0 \le t_{h1} < t_{h2}$. In (21), notations $t_{hj}-0$ and $t_{hj}+0$ stand for left and right limits of the functions $N(t)$ and $B(t)$, i.e represent the time moments immediately before and immediately after the moment t_{hj}, so the equations describe finite jumps, of N by H_j and of B by $W_0 H_j$ at the time moments t_{h1} and t_{h2}. The age of larvae was then measured relative to the latest hatching event,

$$A = \begin{cases} t - t_{h1},\ t_{h1} < t < t_{h2}, \\ t - t_{h2},\ t > t_{h2}. \end{cases} \tag{22}$$

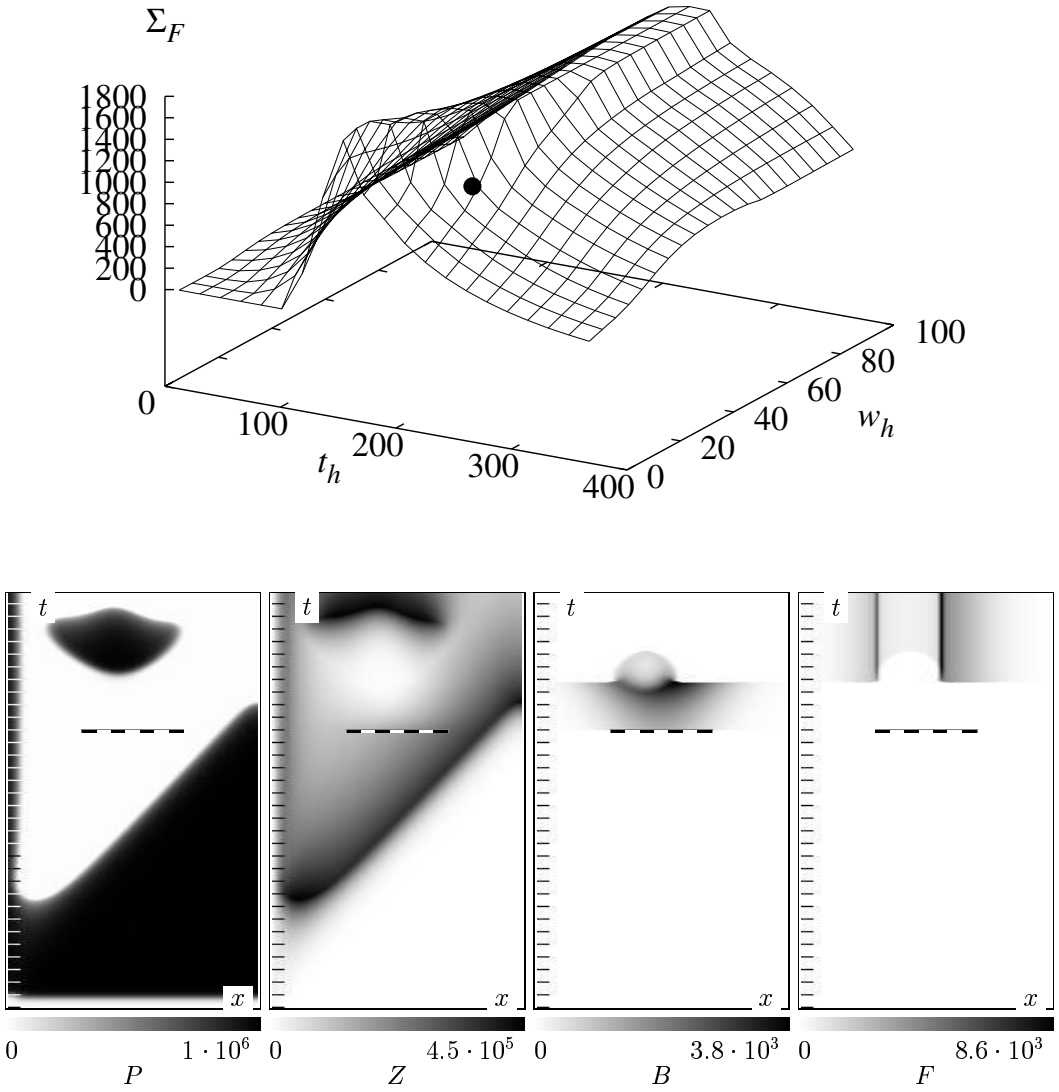

Fig. 9. Recruitment biomass, as function of hatching time t_h and width w_h, for a selected total hatching number, $\Sigma_N = 1240$. "Fair" plankton parameters. Lower panels: evolution of the system corresponding to the parameter choice designated by the filled circle on the above graph.

Figure 10 illustrates the recruitment results for one series of such numerics. There the width and amplitude of hatching were the same for both cohorts, $A_h = 100\,\mathrm{N/m^3}$ and $w_h = 3\,\mathrm{km}$, the first cohort was located at $x_{h1} = 30\,\mathrm{km}$ and hatched at $t_{h1} = 10\,\mathrm{d}$, and localisation x_{h2} and timing t_{h2} of the hatching of the second cohort varied. Thus the resulting graph of $\Sigma_F(x_{h2}, t_{h2})$ shows clear traces of the wave triggered by the first cohort. The lower panels on Figure 10 demonstrate that the first cohort of larvae has completely died out, so the whole recruitment is from the second cohort, which shows mainly a bimodal distribution typical for this relatively weak plankton distrubtion.

3.7 Evolution in two dimensions

Two-dimensional numerical experiments were performed in a rectangular domain $(x, y) \in [0, x_{\max}] \times [0, y_{\max}]$, similarly to those in 1D. The zooplankton

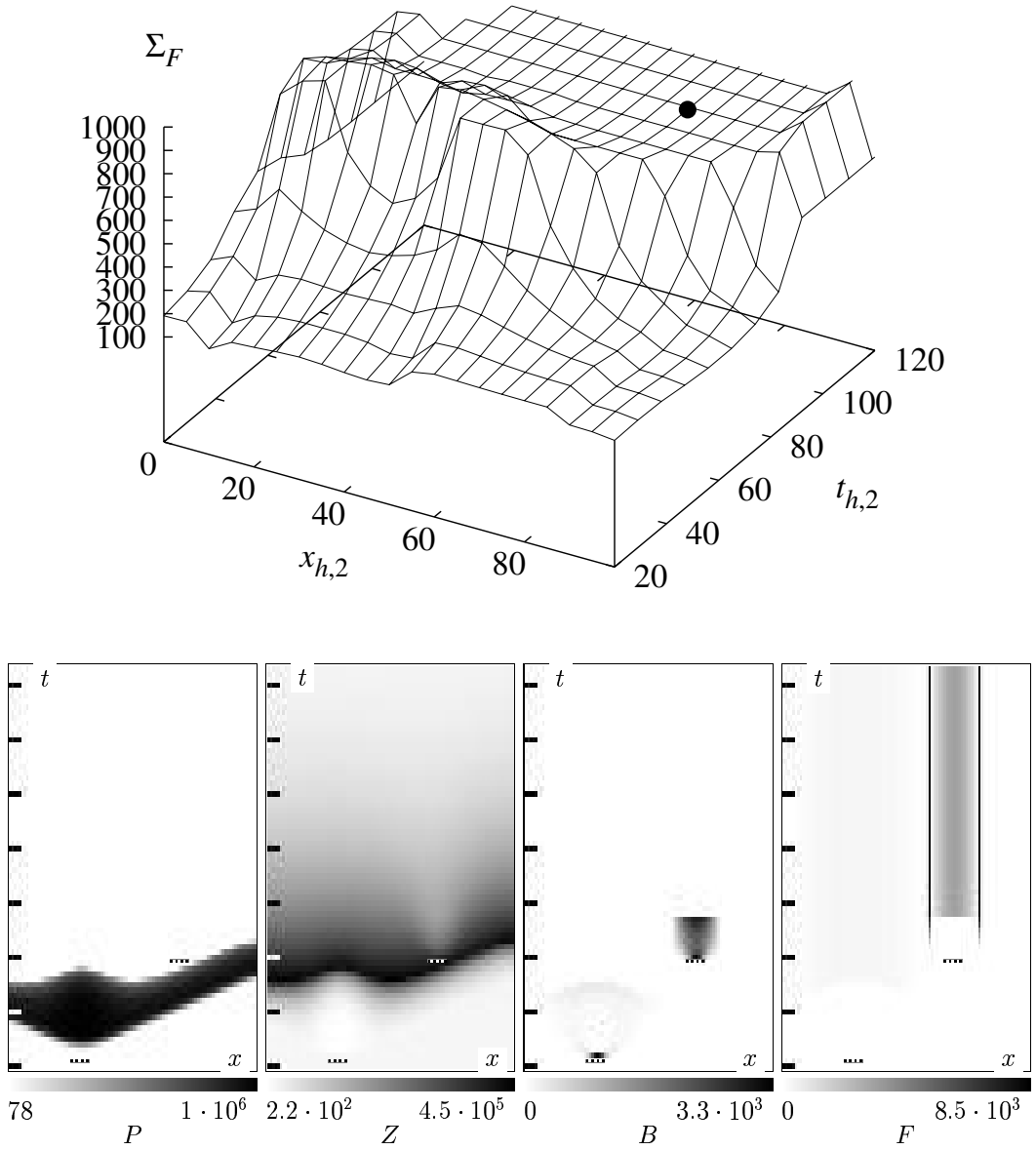

Fig. 10. Recruitment biomass, as function of hatching time t_{h2} and location x_{h2} of the second batch. "Fair" plankton parameters. Lower panels: evolution of the system corresponding to the parameter choice designated by the filled circle on the above graph. Note that the timescale here is different from other figures: the tics on t axis are still in every 10 days.

invasion wave was initiated on the left boundary of the system, $x = 0$. To make computations more interesting we set initial conditions for larvae in the form of a few Gaussian batches:

$$N(t_h, x) = A_h \sum_{j=1}^{3} \exp\left(-\left(\frac{(x - x_{hj})^2 + (y - y_{hj})^2}{w_h^2}\right)\right). \tag{23}$$

As opposed to 1D experiments, which we performed massively to reveal any interesting features in dependences of recruitment upon various parameters, 2D experiments were performed more sparingly, to see if any new patterns compared to the 1D case may occur. In a majority of situations, nothing unexpected happened: recruitment pattern followed that of hatching, modulo

availability of the zooplankton during the larvae growth.

Interesting events occur, as in 1D, when the plankton is so weak that the larvae dynamics significantly affects it. In the 1D case, this led to a bimodal pattern of metamorphosis after a unimodal pattern of hatching. An example of the corresponding situation in 2D is illustrated in Figure 11, which was obtained for $\{(x_{hj}, y_{hj})\} = \{(20, 15), (50, 15), (80, 15)\}$ (km), $A_h = 100\,\mathrm{N/m^3}$, $w_h = 5\,\mathrm{km}$ and $t_h = 162\,\mathrm{d}$, in zooplankton invasion wave in the "modest" plankton subsystem.

One might suppose that this bimodal metamorphosis pattern in 1D is due to diffusion-driven instability during the metamorphosis. However, this explanation should have produced localised spots of metamorphosis in 2D, whereas the observed patterns are different, "halo" type; see fig. 11. This suggests a much more prosaic explanation, to do with the Cushing and Horwood (1994) non-monotonic stock-recruitment dependence. That is, for a Gaussian hatching distribution, in the central region the larvae concentration may be too large; they eat out all zooplankton before reaching metamorphosis, and thus starve out. Far from the central region, they are too few in the beginning, so there are few of them at metamorphosis. Only at some medium radii is the initial larvae concentration close to the optimum, so producing substantial larvae biomass at metamorphosis. This of course, to a certain extent, is moderated by the diffusion.

The figure shows a numerical experiment with three hatching sites: ahead, on the crest, and on the wake of the propagating wave of zooplankton propagating into the abundant phytoplankton. The site ahead does not produce anything as all larvae instantly starve out. The site on the crest of the zooplankton wave produces a substantial number of larvae; this makes a "hole" in the zooplankton distribution, which limits the following growth of larvae in the centre of that site, thus leading to the halo pattern of metamorphosis. This does not produce the phytoplankton bloom wave as the amount of phytoplankton at the crest of the wave is not sufficient. The site on the wake produces a smaller amount of larvae as the amount of zooplankton is much smaller. The phyto/zooplankton system there is close to equilibrium, and so the consumption of zooplankton by larvae leads to development of a phytoplankton bloom followed by zooplankton growth, i.e. the excitation wave.

3.8 Comparative importance of parameters for the recruitment

To find out which of the three parameters r_P, γ and $P_{\max}$ has the most important effect on the observed difference in behaviour, we have studied dependence of the maximal recruitment biomass Σ_F on these parameters, in different combinations. This was done for larvae development in the plankton Fisher waves, such as those illustrated on Figures 2–5. For each combination of the three parameters, we calculated the maximal possible recruitment for the whole range of the hatching times t_h and intensities A_h.

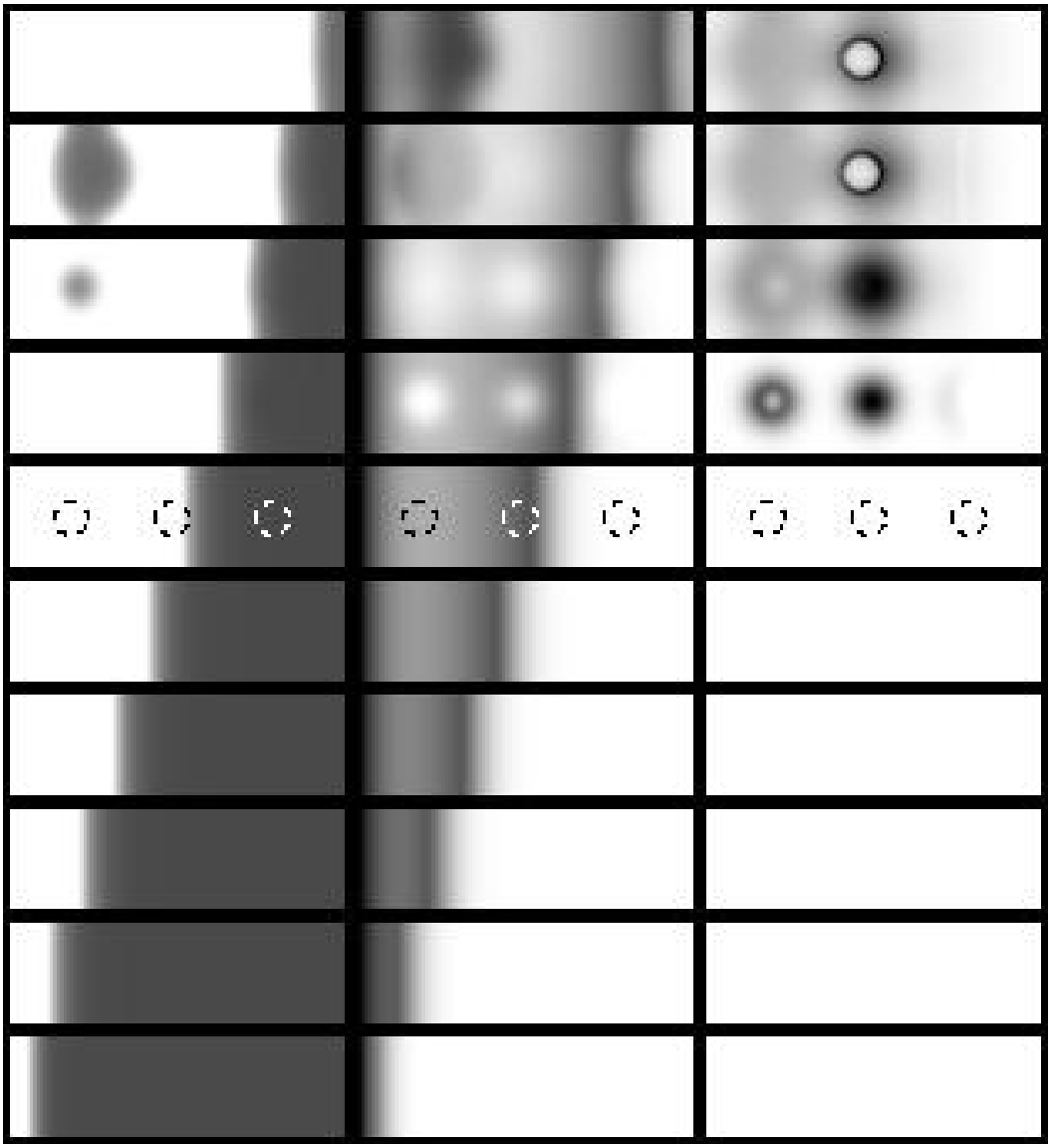

Fig. 11. Hatching in 3 sites in 2D propagating zooplankton invasion wave, leading to a "halo" recruitment patterns. Time: bottom to top, snapshots with the interval of 25 days, starting from day 25. Left column: phyto; middle column: zoo; right column: larvae+metamorphosed fish biomass (normalised); white is 0, black is max. The hatching time is $t_h = 162$. The dashed contrasting circles on the sixth row of panels ($t = 150$) designate the hatching sites; the radius of the circles corresponds to w_h. "Modest" plankton parameters.

The results are summarised on Figure 12. It is clear that the major crucial role belongs to the phytoplankton carrying capacity $P_{\max}$, which is no surprise since in these series this parameter changed by a factor of 30 while the other two remained within the same order of magnitude.

However, as is obvious from the graph $P_{\max} = 3 \cdot 10^6$, a 30-fold increase of the carrying capacity from the weak plankton of Truscott and Brindley (1994) would be sufficient to produce the same recruitment as in Cushing and Horwood (1994). Indeed, an increase from $1 \cdot 10^5$ to $5 \cdot 10^5$ already displays enormous increase ($\times 50$) in recruitment, suggesting that the increase in $P_{\max}$

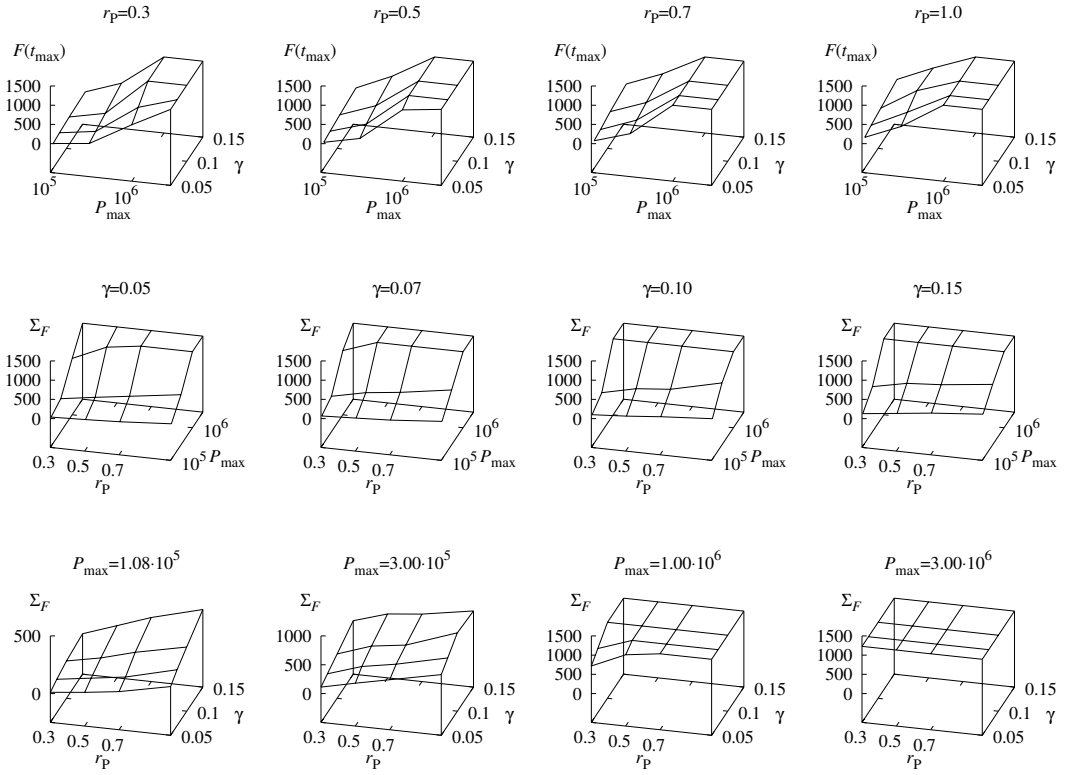

Fig. 12. Recruitment biomass Σ_F as function of r_P, γ and $P_{\max}$, in the numerical experiments as shown on Figures 2–5.

above some threshold level is the crucial factor in recruitment. This is all the more striking if we recall that the recruitment here is the average over the whole medium, rather than the maximal one.

It appears that the situation in the spatially structured model is different from the spatially uniform model where all three parameters r_P, $P_{\max}$ and γ are important in achieving high recruitment. In the 1D model, the average recruitment, and especially its peak, depend strongly only on $P_{\max}$.

4 Discussion

The spatially structured model considered here has demonstrated some qualitatively new features, compared to the unstructured and age-structured models considered before (Biktashev et al., 2003).

The phytoplankton-zooplankton interaction in the spatially distributed Truscott-Brindley model (in absence of larvae) is able to sustain propagating waves, which may be considered as a simplest dynamic model of plankton patchiness. As the larvae development is extremely sensitive to the copepod abundance, the recruitment success depends on the localisation and timing of the hatching site with respect to such waves. The waves may be of different kinds; but the exact mechanism of the waves is of little importance, only zooplankton availability is of importance.

A distinctive feature of the unstructured zooplankton-larvae model of Cushing and Horwood (1994) was a bell-shaped dependence of the recruitment success on spawning stock. Obviously, if very few larvae have spawned, only few of them can reach maturity; on the other hand, too many larvae from the beginning may exhaust the zooplankton availability before larvae reach maturity, and so increase of stock then leads to decrease of recruitment. This feature was more or less preserved from the unstructured model involving phytoplankton dynamics (Biktashev et al., 2003). In the present study, however, we find that if the size of the hatching site is less than the typical size of the zooplankton patch (i.e. width of the zooplankton wave), and the plankton subsystem is strong enough, then this inverse stock-recruitment dependence can be to a considerable extent reduced, as the local exhaustion of the zooplankton at the larvae site can be alleviated by diffusion of plankton from neighbouring sites. In this situation, when the initial concentration of larvae is too high to be supported by locally available plankton, the spatial distribution of the larvae reaching the metamorphosed stage has distinct features: they tend to concentrate on the edges of the hatching site, where the balance between the larvae and zooplankton is optimal from the viewpoint of the unstructured Cushing-Horwood mechanism because of the action of diffusion during the larvae growth time. In our idealised 1-dimensional and 2-dimensional models this was a sharp bimodal or annulus-shaped distribution, respectively; one can expect in reality, with account of advection and environment inhomogeneity, that the perfect circles may be deformed and the most robust feature would be a stripe shape of the recruited fish distribution, on the edge of a zooplankton patch.

When the phyto/zooplankton subsystem is relatively weak the larvae development may influence the dynamics of the plankton subsystem. This feedback can lead to new phenomena. One is that an appropriately timed hatching can extinguish a whole zooplankton patch or temporarily stop a zooplankton wave from propagating. Another effect is that, in the absence of the plankton wave, hatching of larvae may itself initiate such a wave, through local and temporal decrease of zooplankton grazing pressure on the phytoplankton, subsequently triggering the phytoplankton bloom through a prey-escape mechanism.

A nontrivial consequence of the larvae-initiated plankton waves is the possibility of cooperative effects between different larvae batches. For instance, the phyto/zooplankton wave initiated by a batch of spawned larvae, although useless for this same batch, may be beneficial for another batch later in time and in another place, where and when the zooplankton component of the wave initiated by the first batch arrives. This possibility may influence the spawning strategy of the fish.

The feasibility of any of the above conclusions depends, of course, on the assumptions made in the model. In this study, we have mostly analysed just four selected parameter sets, within the range consistent with data available in the literature. Thus the possibility of a wider variety of phenomena that may occur at other values of parameters cannot be excluded. Other features, such as seasonal and geographical variations of the parameters, may also have

significant effect. As noted in James et al. (2003), a phytoplankton bloom initiated exclusively by larvae is unlikely; however, the effect of larvae may enhance the effect of the season and quicken the onset of the phytoplankton bloom; in this situation, cooperative effects between time- and space-separated spawning batches may well take place.

5 Acknowledgement

We are grateful to Prof. A.V. Holden for providing computational facilities for this work and to Dr J. Horwood for stimulating discussions. This work was supported by NERC project GR3/11671.

References

Abraham, E. R., 1998. The generation of plankton patchiness by turbulent stirring. Nature 391, 577–580.

Bainbridge, R., 1957. Size, shape and density of marine phytoplankton concentrations. Biol. Review 32, 91–115.

Biktashev, V. N., Brindley, J., Horwood, J. W., 2003. Phytoplankton blooms and fish recruitment rate. Journal of Plankton Research 5 (1), 21–33.

Cushing, D. H., Horwood, J. W., 1994. The growth and death of fish larvae. Journal of Plankton Research 16, 291–300.

de Roos, A. M., McCawley, E., Wilson, W. G., 1998. Pattern formation and the scale of interaction between predators and their prey. Theor. Pop. Biol. 52, 108–130.

Fisher, R. A., 1937. The wave of advance of advantageous genes. Phil. Trans. Roy. Soc. Lond. B 7, 355–369.

Flierl, G. R., Davis, C. S., 1993. Biological effects of Gulf-Stream meandering. J. Marine Res. 51, 529–560.

Folt, C. L., Burns, C. W., 1999. Biological drivers of zooplankton patchiness. Trends Ecol. Evol. 14, 300–305.

Gurney, W. J. C., Veitch, R., 2000. Self-organisation, scale and stability in a spatial predator-prey intraction. Bull. Math. Biol 62, 61–86.

Heath, M. R., Gallego, A., 1998. Bio-physical modeling of the early life stages of haddock, *melanogrammus aeglefinus*, in the North Sea. Fisheries Oceanography 7, 110–125.

James, A., Pitchford, J. W., Brindley, J., 2003. The relationship between plankton blooms, the hatching of fish larvæ and recruitment. Ecological Modelling 160 (1–2), 77–90.

Kolmogoroff, A., Petrovsky, I., Piscounoff, N., 1937. Étude de l'équation de la diffusion avec croissance de la quantité de matière et son application à un problème biologique. Moscow Univ. Bull. Math. 1, 1–25.

Martin, A. P., Richards, K. G., 2001. Mechanisms for vertical nutrient transport within a North Atlantic mesoscale eddy. Deep-Sea Res. II 48, 757–773.

Matthews, L., Brindley, J., 1997. Patchiness in plankton populations. Dynamics and Stability of Systems 12, 39–59.

McGillicuddy Jr, D. J., Robinson, A. R., 1997. Eddy-induced nutrient supply and new production in the Sargasso Sea. Deep-Sea Res. I 44, 1427–1450.

Miller, D. G. M., Hampton, I., 1989. Biology and ecology of the antarctic krill (*Euphausia superba Dana*): a review. In: BIOMASS 9. Scott Polar Research Institute (SCAR/SCOR), Cambridge, England, pp. 1–166.

Neufeld, Z., Haynes, P., Garçon, V., Sudre, J., 2002. Ocean fertilization experiment may initiate a large scale phytoplankton bloom. Geophys. Res. Lett. 29 (11), 1534.

Okubo, A., 1980. Diffusion and ecological problems: mathematical models. Vol. 10 of Biomathematics. Springer Verlag, Berlin, Heidelberg, New York.

Oschlies, A., Garçon, V., 1998. Eddie-induced enhancement of primary productivity in a model of the North Atlantic. Nature 398, 266–268.

Oschlies, A., Koeve, W., Garçon, V., 2000. An eddy-permitting coupled physical biological model of the North Atlantic, 2. ecosystem dynamics and comparison with satellite and JGOFS local studies data. Global Biogeochemical Cycles 14, 499–523.

Pitchford, J. W., Brindley, J., 2001. Prey patchiness, predator survival and fish recruitment. Bull. Math. Biol. 63, 527–546.

Siegel, D. A., Jr., D. J. M., Fields, E. A., 1999. Mesoscale eddies, satellite altimetry and new production in the Sargasso Sea. J. Geophys. Res. 104, 13359–13379.

Steele, J. H., 1978. Some comments on plankton patches. In: Steele, J. H. (Ed.), Spatial pattern in plankton communities. Plenum Press, New York and London, pp. 1–20.

Steele, J. H., Henderson, E. W., 1981. A simple plankton model. The American Naturalist 117, 676–691.

Steele, J. H., Henderson, E. W., 1992a. The role of predation in plankton models. Journal of Plankton Research 14, 157–172.

Steele, J. H., Henderson, E. W., 1992b. A simple model for plankton patchiness. Journal of Plankton Research 14, 1397–1403.

Strass, V. H., 1992. Chlorophyll patchiness caused by mesoscale upwelling at fronts. Deep-Sea Res. A 39, 75–96.

Talbot, J. W., 1976. Diffusion data. Fisheries research technical report 28, MAFF Directorate of Fisheries Research, Lowestoft.

The PRIME Community, 2001. The PRIME study. Deep-Sea Res. II 48 (4–5).

Truscott, J. E., Brindley, J., 1994. Equilibria, stability and excitability in a general class of plankton population models. Phil. Trans. Roy. Soc. London A 347, 703–718.

Venrick, E. L., 1990. Mesoscale patterns of Chlorophyll-A in the central North Pacific. Deep-Sea Research A 37, 1017–1031.

A Appendix: table of notations

Notation	Std (init) val	Units	Meaning
Independent variables			
t		d	time
x		km	space
y		km	space
Dynamic variables			
$P(t,x)$	$4 \cdot 10^3$	$\mu\text{g} \cdot \text{N/m}^3$	phytoplankton biomass concentration
$Z(t,x)$	$4 \cdot 10^3$	$\mu\text{g} \cdot \text{N/m}^3$	zooplankton biomass concentration
$N(t,x)$	1	N/m^3	larva number per volume
$A(t,x)$	0	d	larvae age
$B(t,x)$	1	$\text{N} \cdot \mu\text{g/m}^3$	larva biomass per volume
$F(t,x)$	0	$\text{N} \cdot \mu\text{g/m}^3$	metamorphosed fish biomass per volume
Model parameters			
$P_{\max}$	$1.08 \cdot 10^5$	$\mu\text{g} \cdot \text{N/m}^3$	TB phytoplankton saturation constant
r_P	0.3	d^{-1}	TB phytoplankton maximal growth rate
r_Z	0.7	d^{-1}	TB zooplankton maximal grazing rate
P_*	$5.7 \cdot 10^3$	$\mu\text{g} \cdot \text{N/m}^3$	TB zooplankton grazing half-saturation constant
γ	0.05		TB zooplankton grazing efficiency
μ_Z	0.012	d^{-1}	TB zooplankton mortality and predation rate

Notation	Std (init) val	Units	Meaning
k	0.0154	$\mu g^{-\nu}$	CH larvae weight-search volume coefficient
ν	0.2234		CH larvae weight-search volume exponent
n	0.67		CH larvae weight-metabolic cost exponent
r_L	0.12	d^{-1}	CH maximal larva growth rate
σ	2.6	μg^{1-n}	CH larvae weight-metabolic cost coefficient
j	0.002		CH larvae maximal digestive coefficient exponent
$\beta_{\max}$	0.48		CH larvae max digestive coefficient
$\beta_{\min}$	0.135		CH larvae minimal (initial) digestive coefficient
μ_L	0.089	d^{-1}	CH larvae initial mortality to predation rate
b	0.005	d^{-1}	CH larvae mortality to predation decrease rate
C_S	0.001	d^{-1}	CH larvae starvation rate coefficient
ν_S	1		CH larvae starvation rate exponent
A_T	100		CH larvae metamorphosis age
C_A	1	d^{-1}	CH larvae metamph-age rate coefficient
Δ_A	10	d	CH larvae metamorphosis age spread
W_T	3165	μg	CH larvae metamorphosis weight
C_W	1	d^{-1}	CH larvae metamph-wgt rate coefficient

Notation	Std (init) val	Units	Meaning
Δ_W	10	μg	CH larvae metamorphosis weight spread
Computation parameters			
D	0.864	km^2/d	turbulent diffusivity
t_h	5	km	hatching time
$t_{\max}$	256	d	total calculation time
Σ_F	0	N $\cdot$ μg $\cdot$ km/m^3	total hatching recruitment biomass
$x_{\max}$	100	km	domain size
W_0	33	μg	initial larva weight
w_h	5	km	hatch zone width
x_h	50	km	hatch zone center
A_h	0	N/m^3	hatch maximal intensity
t_h	128	d	time of hatching
Σ_N	0	N $\cdot$ km/m^3	total hatching number
$y_{\max}$	30	km	domain size
y_h	various	km	hatch zone center
Auxiliary functions			
G			TB amount phyto eaten by zoo per zoo μg per day
W		μg	CH average weight of individual larvae
R		μg	CH larvae ration per larvae capita per day
H		N/m^3	local hatching intensity